

Contents lists available at ScienceDirect

Innovative Food Science and Emerging Technologies

journal homepage: www.elsevier.com/locate/ifset





Exposure to 222 nm far UV-C effectively inactivates planktonic foodborne pathogens and inhibits biofilm formation

Hanyu Chen, Carmen I. Moraru

Department of Food Science, Cornell University, Ithaca, NY 14850, USA

ARTICLE INFO

Keywords:
222 nm krypton chloride excimer lamp
Foodborne pathogen
Inactivation
Biofilm inhibition
Bacterial resistance, chemical sanitizer

ABSTRACT

This study investigated the performance of a 222 nm far-UV-C krypton-chloride excilamp for inactivation of major foodborne pathogenic and spoilage bacteria in thin liquid films (TLF, 1.2 mm thickness), on solid stainless steel surfaces (SS), and against biofilm formation on SS. Both gram-positives (*Listeria monocytogenes, Staphylococcus aureus*) and gram-negatives (*Escherichia coli* O157:H7, *Pseudomonas aeruginosa*) (10^9 CFU/mL starting concentration) were exposed to 222 nm light at cumulative doses of up to 354 mJ/cm². Significant (P < 0.05) reductions (1.4–5.1 log CFU) were found for all bacteria, and inactivation kinetics was described well by the Weibull model ($0.77 \le R^2 \le 0.95$). Substrate type (*i.e.*, TLF *vs.* SS) substantially impacted treatment efficacy. No detectable resistance of *L. monocytogenes* was developed after repeated exposure to 222 nm in TLF. The 222 nm treatment also effectively minimized biofilm formation and growth by *S. aureus* and *P. aeruginosa* and increased the surviving cells' susceptibility to sodium hypochlorite by at least 2 fold.

Industrial relevance: This work demonstrates that 222 nm krypton-chloride excilamps can be used to effectively inactivate planktonic bacteria and inhibit biofilm formation and growth. This recommends them for use as novel nonthermal light-based systems for mitigation of pathogens and biofilms in a range of applications, including food processing, food service, and clinical environments.

1. Introduction

The use of ultraviolet (UV) light for inactivating microorganisms is well established (Cheng et al., 2020; de Silerio-Vázquez, Núñez-Núñez, Proal-Nájera, & Alarcón-Herrera, 2022; Gayán, Condón, & Álvarez, 2013; Kim, Kang, & Schottel, 2018). Traditional UV disinfection systems use low-pressure (LP) mercury (Hg) germicidal lamps with peak emission at 254 nm, in the UV-C range. While effective against microorganisms, exposure to this wavelength represents a human health hazard, as it can cause damage to cells and tissues in the human skin and eyes. Mercury lamps also pose environmental risks as they are constructed from a fragile quartz material that contains toxic mercury, and thus require careful handling and proper disposal procedures. Furthermore, these lamps have a short lifetime, a long warm-up time, and a dependence of radiation intensity on temperature, which limit their applicability (Cheng et al., 2020).

Excimer lamps, or excilamps, are viewed as a promising alternative to conventional UV-C lamps due to the absence of mercury, fast warm-up, long lifetime, wavelength-selectivity, and design flexibility

(Rahmani, Bhosle, & Zissis, 2009). These novel sources of UV light generate radiation because of the dissociation of either excimers, which are excited dimers of molecules that either consist of the same atoms (e. g., Kr_2), or of exciplex molecules (so-called exciplex = excited complex) in case of hetero-atomic molecules (e.g., KrCl). Depending on the type of rare gas used to excite the excimer molecules, excimer lamps can generate nearly monochromatic radiation, ranging from 172 to 345 nm. In recent years, researchers explored the germicidal efficacy of excilamps and determined that various types (Xe2-, KrCl-, NeXe-, and XeBrexcilamps with maximum emission at 172, 222, 270, and 282 nm, respectively) were shown to be effective for the inactivation of pathogens (Ha, Lee, & Kang, 2017; Hessling, Haag, Sieber, & Vatter, 2021; Kang, Kim, & Kang, 2018). Among them, KrCl excilamps emitting far-UV-C light with a peak wavelength at 222 nm were found to have the highest inactivation efficiency. Yin et al found that inactivation of E. coli O157:H7 by 222 nm radiation (KrCl-lamp) was higher than by 254 nm (LP Hg) or 282 nm (XeBr-lamp) in apple juice (Yin, Zhu, Koutchma, & Gong, 2015). Wang et al reported that inactivation of Bacillus subtilis spores following exposure at 222 nm (KrCl-lamp) was higher than for

E-mail address: cim24@cornell.edu (C.I. Moraru).

 $^{^{\}ast}$ Corresponding author.

254 nm (LP Hg) and 172 nm (Xe2-lamp) (Wang, Oppenländer, El-Din, & Bolton, 2010). Ha *et al* found that intermittent exposure of 222 nm (KrCl) light led to a maximum 3.92 log reduction of *E. coli* O157:H7, 4.70 log reduction of *Salmonella Typhimurium*, and 3.03 log reduction of *L. monocytogenes* in water suspensions (Kang & A.-J.-W. H. A.-D.-H, 2018). These findings suggest that 222 nm excilamps can be considered a potential alternative of 254 nm UV-C mercury lamps for inactivation of foodborne pathogenic bacteria.

One essential advantage of 222 nm treatment is that studies to date suggest that this wavelength does not cause the human health issues associated with direct exposure to conventional 254 nm UV-C germicidal light (Buonanno, Welch, Shuryak, & Brenner, 2020; Hessling et al., 2021; Welch et al., 2018). This is because far-UV-C light (207–222 nm) has very limited penetration depth and can only penetrate less than a few micrometers in biological materials, and thus cannot reach human cells in skin or eyes, nor be absorbed in the skin stratum corneum or the ocular tear layer (Welch et al., 2018). Nonetheless, because bacteria and viruses are micrometric or submicrometric in size, 222 nm light can penetrate and kill them.

Far-UV-C light was reported to induce microbial damage in two ways: 1) by affecting cellular enzymes and membrane lipids in microorganisms, because amino acids and phospholipids have an absorption peak at 222 nm wavelength; 2) by inducing generation of reactive oxygen species (ROS) in the ubiquitous chromophores in the microbial cells; therefore, even though DNA does not absorb the 222 nm wavelength very well, it can be indirectly but significantly damaged by ROS (Kang et al., 2018). To this date, most studies involving 222 nm treatments have focused on the treatment of air or water disinfection where bacteria were suspended in liquid substrates, and knowledge of the antimicrobial effectiveness of 222 nm light on solid substrates and in biofilms is limited. To address this knowledge gap, this study aims to assess the bactericidal effect of 222 nm far-UV-C light against several major food pathogens, both in liquid and solid substrates, and to evaluate the effect of the substrate on inactivation kinetics and treatment effectiveness. The effect of 222 nm light treatment on biofilm formation and growth on abiotic surfaces, the potential development of bacterial resistance to 222 nm light exposure over multiple growth cycles, and the effect of 222 nm pre-treatment on the subsequent chemical susceptibility of bacteria were also investigated, to provide a comprehensive assessment of the effectiveness and possible limitations of 222 nm light in many areas that affect human health and life, including food processing and handling, healthcare, and clinical environments.

2. Materials & methods

2.1. Bacterial cultures

The bacterial strains used in this study were *L. monocytogenes* serotype 1/2a strain 10403 s, *E. coli* serotype O157:H7 ATCC43895, *S. aureus* ATCC9144, and *P. aeruginosa* ATCC15442, obtained from American Type Culture Collection (Manassas, VA). Prior to the experiments, all cultures were streaked onto tryptic soy agar (TSA) from frozen stock ($-80~^{\circ}$ C) and incubated for 24 h at 37 $^{\circ}$ C. A single isolated colony was then transferred into 3 mL of tryptic soy broth (TSB) for passage one (37 $^{\circ}$ C, 24 h). Thirty μ L of grown passage one culture was transferred to fresh 3 mL TSB for passage two (37 $^{\circ}$ C, 18 h). Bacteria suspension in early stationary phase was centrifuged at 5000 RPM (1957 \times g) for 10 min at 21 $^{\circ}$ C, and the pellet was resuspended in Butterfield Phosphate Buffer (BPB, pH = 7.2) for three times total to ensure minimal remnants of TSB in the final bacteria suspension. The initial inoculum level was about 10^{9} CFU/mL for all strains.

2.2. 222 Nm far-UV-C excilamp treatment setup

All inactivation experiments were performed using a Dielectric Barrier Discharge (DBD) excimer lamp filled with Krypton Chloride

(KrCl) gas mixture (DF28B-20 W 24 V, Sterilization Center, Oak Park, IL), with an output power of 24 W and maximum emission at 222 nm. The excilamp had cylindrical geometry (30.7 \times 11.7 \times 3.8 cm), and was covered by a metal case with a UV exit window of 50 cm² area (10 \times 5 cm). The apparatus was kept in a 21 \pm 2 $^{\circ}$ C low temperature incubator at all times, to prevent any heating of the samples during exposure to the light source, and to eliminate any disturbance from ambient lighting. The rectangular lamp was set in a fixed position, at 15.5 cm directly above the target surfaces, to provide a good balance between intensity of irradiance and the homogeneity of the light distribution, giving an approximate irradiance of 0.236 mW/cm² at the targeted surfaces. Several treatment durations were chosen to deliver different cumulative dosages of 222 nm light: 30 s, 60 s, 120 s, 180 s, 300 s, 600 s, 1000 s, 1200 s, and 1500 s, corresponding to cumulative fluences of 7.1 mJ/ cm², 14.2 mJ/cm², 28.3 mJ/cm², 42.5 mJ/cm², 70.8 mJ/cm², 141.6 mJ/cm², 236.0 mJ/cm², 283.2 mJ/cm², and 354.0 mJ/cm² respectively.

2.3. Bacterial inactivation by 222 nm far-UV-C light on different substrates

2.3.1. Treatment on nutritive agar plate

E. coli, L. monocytogenes, S. aureus, and P. aeruginosa cultures were streaked in parallel lines on nutritive TSA plates of 100 mm in diameter. Half of each plate was covered with aluminum foil, to divide the surface of the plate and the bacterial streaks into an "Exposed" section and a "Covered" section (S1), and then exposed to the 222 nm light for a specified duration (30 s to 180 s). After the treatment, plates were incubated at 37 °C for 24 h for preliminary qualitative evaluation of bacteria inactivation efficacy. The qualitative results are shown in the Supplementary Information (S1), and demonstrate a significant reduction in the culturable population of all four tested strains on nutrientrich surfaces exposed to 222 nm light over 180 s continuous exposure, confirming the bactericidal effects of 222 nm treatments.

2.3.2. Treatment of thin liquid films

To mimic contaminated standing water in food processing and handling environments, 1 mL of bacteria suspension was transferred into Nunc Lab = TekTM II 1 well Chamber SlideTM (17 mm \times 48 mm, Fisher Scientific, Rochester, NY) in the form of a thin liquid film (TLF). Prior to use, the chambers were soaked in 70% ethyl alcohol for 24 h for decontamination, followed by 2 h of drying in a biosafety cabinet to evaporate the remaining ethyl alcohol. The bacteria suspensions were allowed to equilibrate for 3 min prior to the 222 nm light exposure. The effect of strains on light inactivation kinetics was investigated by exposing 1 mL of liquid film (thickness = 1.2 mm) containing L. monocytogenes, E. coli, S. aureus, or S. epidermidis, for the durations specified previously. The survivors from both light-treated and untreated control samples were enumerated using the standard plate counting method on tryptic soy agar (TSA). Plates were incubated at 37 °C for 24 h, after which the survivors were enumerated, and results were reported as colony forming units (CFU/mL). Log reduction was calculated using the following equation:

$$Log \ reduction = Log(N/N_0) \tag{1}$$

Where N_0 and N are bacterial counts (in CFU per mL of suspension) before and after 222 nm light treatment, respectively. The detection limit for all strains in TLF experiments was 25 colonies per streaked agar plate.

To assess the potential development of bacterial resistance to the 222 nm treatment, the light treatment of TLF was performed for up to five exposure-growth cycles, using L. monocytogenes as a challenge microorganism. Three cumulative doses (70.8 \pm 0.6 mJ/cm², 141.6 \pm 1.2 mJ/cm², 236.0 \pm 2.0 mJ/cm²) were used for each exposure-growth cycle to determine if there was any difference in log reduction at different cumulative doses. Following the light treatment, the aforementioned plate counting and enumeration methods were used, and

plates were incubated at 37 $^{\circ}$ C for 24 h to allow for growth of surviving cells. The light treatments were then repeated on a suspension containing the newly grown bacteria solution, using the surviving cells from the previous cycle.

2.3.3. Treatment of solid stainless steel surfaces

Food-grade stainless steel (SS) coupons ($40\,\text{mm} \times 100\,\text{mm}$) with a glass bead blasted finish ($R_a=0.78\,\mu\text{m}$) were used to simulate polished SS surfaces commonly encountered in food handling and medical environments. To remove any surface chemical contaminants, the SS coupons were sequentially submerged in a rotating bath ($100\,\text{RPM}$) of 95% acetone (Fisher Scientific, Rochester, NY), 95% ethyl alcohol, and deionized water, for $10\,\text{min}$ at each step. The coupons were then autoclaved ($15\,\text{min}$, $121\,^{\circ}\text{C}$) in individually sealed sterilization pouches to kill any potential microbial contaminants. The SS coupons prepared as described above exhibited a mean water contact angle of $62.2\pm3.3^{\circ}$ (hydrophobic behavior) as determined by a static sessile drop method with a Ramé-Hart 500 goniometer (Ramé-Hart Inc., Succasunna, NJ, ISSA).

For inoculation, a total of 1 mL bacteria suspension was deposited on the SS surfaces as 20 evenly spaced droplets of 50 µL each. The inoculated coupons were then left to equilibrate in a laminar flow hood (21 °C, relative humidity of 17%) for 3 min before being subjected to the light treatments. The SS coupons were then subjected to 222 nm treatments with different cumulative doses, as described before, after which they were individually placed in sterile Whirl-Pak bags with 99 mL BPB and sonicated for 5 min at 40 kHz (Branson 1210 Ultrasonic Cleaner, Branson Ultrasonics, Danbury, CT). This method of recovery was used, since Bjerkan et al showed that ultrasonication (>20 kHz) for 5 min achieved the highest recovery of bacteria from metal plates compared with other commonly used methods such as manual scraping (Bjerkan, Witsø, & Bergh, 2009). Preliminary experiments conducted as part of the present study also showed no effect of the 5 min ultrasonication step on bacterial viability (data not shown). After sonication, the BPB that contained the recovered cells was subjected to serial ten-fold dilutions with sterile BPB, spread plating on TSA plates, and enumeration of CFUs after incubation at 37°C for 24h. The control followed the same recovery and enumeration procedures, except for the absence of the 222 nm treatment. The detection limit for enumeration was 25 cells per TSA plate for all strains. Inactivation effectiveness, expressed in log reduction, was determined using Eq. 1. All light treatments were performed in triplicate, with independently grown bacterial cultures.

2.3.4. Treatment of young biofilms

The method for developing S. aureus and P. aeruginosa biofilms on surfaces was described before (Feng et al., 2015). Briefly, 16-h-old cultures of planktonic cells at a diluted concentration of $\sim 10^9$ CFU/mL were incubated statically at 37 °C for 24 h and 48 h, respectively, then retrieved and evaluated for bacterial attachment. Small food-grade stainless steel coupons ($10\,\text{mm} \times 15\,\text{mm}$) with a glass bead blasted finish ($R_a = 0.78 \, \mu m$) were used in the biofilm experiments. During the biofilm development, coupons were subjected to continuous 222 nm light for up to 48 h. The incident irradiance at the center of coupon was measured to be 0.16 mW/cm² using a calibrated radiometer (ILT-2400, International Light Technologies, Inc., Peabody, MA, USA) set at the 222 nm peak emission wavelength. Beakers (50 mL, Chemglass, Vineland, NJ) made of GE214 fused quartz were used in all biofilm attachment experiments to ensure an average 90% UV transmittance (UVT) across the biofilm structure. All light treatments were performed in a dark incubator to minimize any disturbance from ambient light. Incubation durations of 24 h and 48 h were chosen since it was previously observed that these time points allowed bacteria to attach to surfaces in sufficient numbers for meaningful quantitative assessments, but without significant biofilm formation that may interfere with the quantification of surface biomass (Feng et al., 2015). Surfaces were placed vertically to reflect true attachment and minimize the effect of sedimentation of bacteria on the surface due to gravity. Biofilms in the control groups were grown under the same condition as the experimental groups, without the exposure to 222 nm light. Triplicates of both experimental and control groups were performed with independently grown cultures.

2.4. Chemical susceptibility of the 222 nm light injured cells

The chemical susceptibility of the light-injured S. aureus and P. aeruginosa bacterial cells treated in the biofilm study was tested in a bench-scale sanitation system against 0.02 M sodium hypochlorite (NaCIO), one of the cleaning chemicals most commonly used in food processing environments. The concentration of the NaCIO solution was chosen based on the manufacturer's recommendation for surface cleaning purposes and industry standards for equipment and food contact surface disinfection (Critzer, Science, Wszelaki, Ducharme, & Specialist, 2017). A shaking speed of 75 rpm and soaking time of 1 min at room temperature (21 °C) were chosen to mimic the manual wiping and scraping employed in surface cleaning regimes. Controls consisting of freshly grown bacterial cells without light treatment were subjected to the same sanitizer treatments. At the end of each treatment, concentrated Dey-Engley neutralizing broth (ThermoFisher Scientific, Rochester, NY, USA) was added to the sanitation system to stop the sanitizer reaction. The initial concentration of bacteria was adjusted to 10⁶ CFU/mL in both experimental and control groups, before the chemical susceptibility test.

2.5. Modeling of inactivation kinetics

Microbial inactivation by 222 nm light treatments was modeled by the nonlinear Weibull model (Uesugi, Woodling, & Moraru, 2007):

$$Log_{10}(N/N_0) = \alpha t^{\beta} \tag{2}$$

Where N/N_0 represents the ratio of survivors after treatment over the initial population, α is the scale parameter, which describes the magnitude of \log_{10} change, and β the shape factor, which describes the shape (e.g., concavity) of the inactivation curves. A shape parameter $\beta>1$ describes a concave down curve, $\beta<1$ describes a concave up curve, and $\beta=1$ describes the case of linear inactivation curve. Parameter fitting was conducted by linear regression through the linearized dataset.

2.6. Confocal laser scanning microscopy

The distribution of *S. aureus* and *P. aeruginosa* cells within the young biofilm attached on SS coupons was visualized using a Zeiss LSM 710 confocal microscope equipped with inverted immersion objectives (Carl Zeiss, Jena, Germany), as described before (Cheng & Moraru, 2018). Briefly, the surfaces with attached cells were gently removed from the culture and rinsed in sterile saline solution (0.15 M NaCl) three times to remove any loosely attached cells. The bacterial biomass was labeled with SYTO-9/Propidium iodide (ThermoFisher Scientific, Rochester, NY, USA) to acquire three-dimensional images of live and dead bacteria. For every type of surface, six replicates (two surfaces per each of three independent experiments) were used. On each sampled surface, at least five randomly selected and evenly spaced fields (512 \times 512 μm^2) were scanned. Three-dimensional images of biomass matrices were constructed using the ZEN blue software (version 3.4.91, Carl Zeiss, Jena, Germany).

2.7. Biomass quantification

The total biomass was quantified using COMSTAT2, a computer program designed specifically for this purpose (Heydorn et al., 2000). A threshold value of 3 was assigned to all the individual image stacks. Quantified parameter was biomass accumulation $(\mu m^3/\mu m^2)$, obtained

by dividing the overall biomass volume by the substratum area.

2.8. Scanning Electron microscopy

Visualization of biomass structures was conducted with a Zeiss Gemini 500 field emission scanning electron microscope (SEM), and images acquired with the SmartSEM software (Carl Zeiss, Jena, Germany). Surfaces with biofilm growth were retrieved at 24 h and 48 h of 222 nm exposure and rinsed in saline solution to remove loosely attached cells. The biomass on the SS surfaces was fixed using 2.5% (w/v) glutaraldehyde in 0.05 sodium cacodylate buffer at 4 °C for 2h. Samples were then rinsed with cacodylate buffer for three times, 5 min each time, and subjected to secondary fixation with 1% (w/v) osmium tetroxide in the cacodylate buffer, for 1 h. The fixated samples were rinsed in cacodylate buffer for three times, then dehydrated using gradient ethanol solutions of 25, 50, 70, 95, 100% (ν/ν) for 10 min each, followed by critical point drying with carbon dioxide. Dried surfaces were mounted to SEM stubs and coated with a gold/ platinum (Au/Pd) mix. A voltage of 1.5-3 kV was used during imaging, depending on the sample.

2.9. Statistical analysis

Analysis of variance and *post hoc* Tukey's HSD were used to compare experimental and Weibull calculated inactivation data. Linear regression analysis was used to analyze the presence of potential bacterial resistance trends. A confidence level of 95% was adopted for all statistical tests, which were performed using the statistical software Minitab 2021 and MATLAB 2021.

3. Results & discussions

3.1. Inactivation of bacteria in thin liquid films

Fig. 1 shows the inactivation curves for 222 nm light treatments of planktonic foodborne pathogens suspended in liquid and on solid substrates. Fig. 1a shows the survivor ratios for the 222 nm light treatments of liquid bacterial suspensions of *E. coli, L. monocytogenes, S. aureus* and *P. aeruginosa* with an initial population density of 10^9 CFU/mL and a suspension thickness of 1.2 mm, exposed to at an irradiance of 0.24 mW/cm² for up to 1500 s (354 mJ/cm² cumulative fluence). Overall, the survivor counts for all strains decreased nonlinearly with increasing light dose. The inactivation kinetics of all strains in TLF was determined.

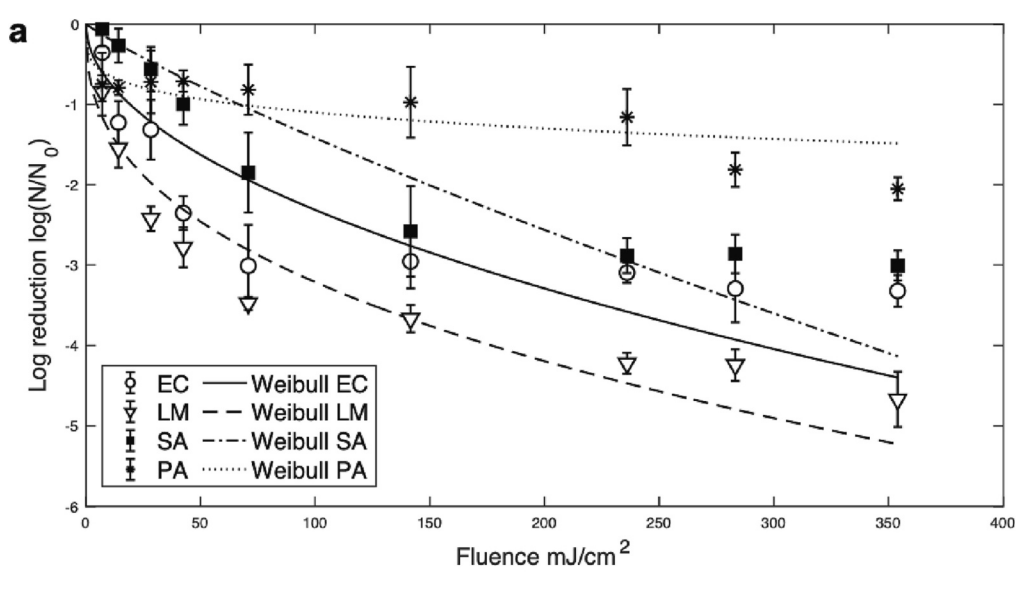
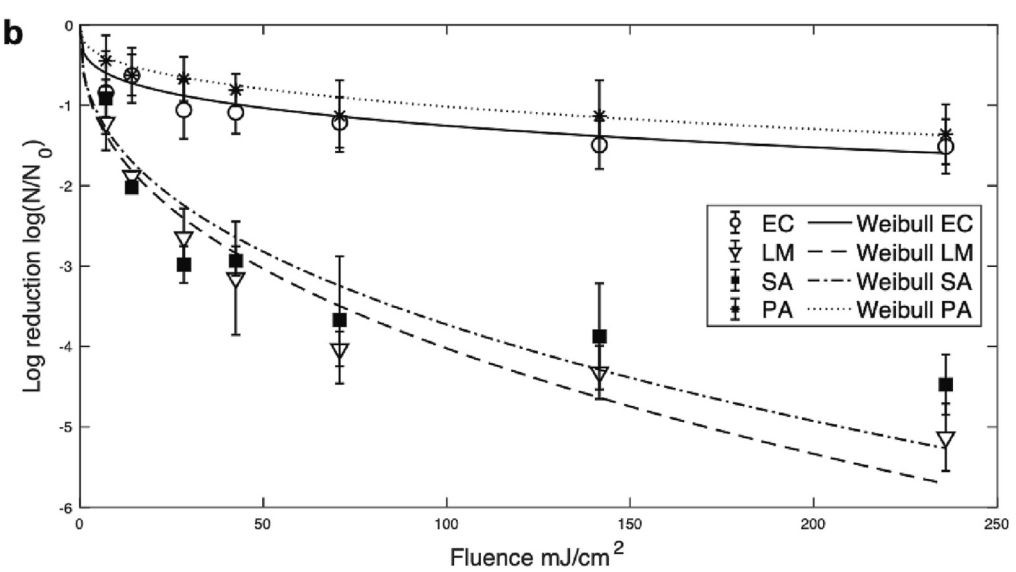


Fig. 1. 222 nm far-UV-C light inactivation kinetics of gram-positive and gramnegative bacteria suspended on different substrates. (a) Comparison between the inactivation kinetics of *E. coli* (EC), *L. monocytogenes* (LM), *S. aureus* (SA), and *P. aeruginosa* (PA) suspended in 1.2mm thick BPB buffer thin liquid films (TLF). (b) Comparison between the inactivation kinetics of *E. coli* (EC), *L. monocytogenes* (LM), *S. aureus* (SA), and *P. aeruginosa* (PA) suspended on solid stainless steel (SS) surfaces.



which allowed a direct comparison of responses by gram-positive and gram-negative strains to the treatment. The inactivation performance by 222 nm light in TLF in this study was less efficient compared with was reported in previous studies (Ha et al., 2017; Janisiewicz, Takeda, Evans, & Camp, 2021; Kang et al., 2018; Matafonova, Batoev, Astakhova, Gómez, & Christofi, 2008; Yin et al., 2015), demonstrated by the lower inactivation levels at similar cumulative fluences. This discrepancy is possibly caused by differences in the experimental setup, including the absence of stirring/shaking of the bacterial suspensions, and a higher initial concentration of bacterial cells before treatment used in this study compared with previous studies. Several studies have claimed that the same dose of 222 nm light could result in higher bacterial and fungal reduction levels compared with 254 nm UV-C light (Ha et al., 2017; Janisiewicz et al., 2021). However, the results of the current study show that a significantly higher dose of 222 nm light is needed to reach similar levels of bacterial reduction as UV-C light treatments. The highest cumulative dose of 222 nm light used here was 354 mJ/cm², about 10 times higher than the 280 nm light dose used to reach 5 log reductions of E. coli and L. monocytogenes under similar TLF conditions, as reported previously by our group (Cheng et al., 2020). Additionally, a higher variability of inactivation levels was observed here for far-UV-C treatments compared with the previous UV-C treatments.

The 222 nm light consistently exhibited a high bactericidal effect against the gram-positive L. monocytogenes and S. aureus suspended in TLF. Fig. 1a shows that L. monocytogenes and S. aureus experienced a fast reduction up to a cumulative fluence of 70.8 mJ/cm² (first 300 s of continuous exposure) followed by a gradual plateau up to a cumulative fluence of 354 mJ/cm² (1500 s), reaching final reductions of 4.7 \pm 0.3 log CFU for L. monocytogenes and 3.0 \pm 0.2 log CFU for S. aureus, respectively. However, the bactericidal effect of 222 nm light on gramnegative E. coli and P. aeruginosa showed higher variability between strains. P. aeruginosa showed high resistance to 222 nm exposure, with a plateau observed as early as 42.5 mJ/cm² cumulative fluence (180 s of exposure) and a lowest final reduction among all strains (2.1 \pm 0.1 log after 354 mJ/cm² cumulative fluence). On the other hand, E. coli showed higher susceptibility to the 222 nm treatment, with a 3.3 \pm 0.2 log reduction achieved after the highest cumulative fluence used (354 mJ/ cm²). The final inactivation levels reached by different bacteria were statistically different from each other (P < 0.05).

To compare the inactivation kinetics by UV-C light and far-UV-C light, the nonlinear Weibull model was used. The Weibull model has been widely used in previous studies to describe inactivation kinetics by light treatments, particularly 250 nm - 280 nm UV-C light, and has shown high accuracy in predicting inactivation (Cheng et al., 2020; Uesugi et al., 2007). The Weibull model was also used in this study to provide a direct comparison between inactivation kinetics by UV-C light and far-UV-C light. The results showed that the Weibull model provided a better fit for gram-positive bacteria, with $R^2 = 0.9$ for both S. aureus and L. monocytogenes. The fit for gram-negative bacteria tested was weaker, with $R^2 = 0.8$ for *E. coli* and $R^2 = 0.7$ for *P. aeruginosa*. The lower accuracy of the Weibull predictive model in 222 nm inactivation of gram-negative strains may suggest a different bacterial behavior of these strains in response to far-UV-C light compared with UV-C light. Additionally, most deviations from the model predictions occurred towards the end of continuous 222 nm treatments under high cumulative doses (i.e., 236–354 $\mathrm{mJ/cm^2}$ cumulative fluence), where the Weibull model tended to overestimate inactivation levels. The lower-than-predicted experimental inactivation data under high cumulative doses may indicate the limit of far-UV-C light penetration power (Welch et al., 2018), leading to an earlier plateau compared with 254 nm UV-C treatments. This finding reinforces our finding that the disinfection efficacy of 222 nm light is lower and slower than of 254 nm UV-C light, which generally fits better with the Weibull model (Cheng et al., 2020; Uesugi et al., 2007). Future research should consider building a more accurate kinetic model for 222 nm far-UV-C inactivation of pathogenic bacteria.

Overall, the results of the TLF experiments show that 222 nm light

treatment effectiveness depends on the bacteria species used, and large differences in inactivation levels can exist among various strains. This needs to be considered when using this treatment in practical applications, to avoid any safety risks.

3.2. Inactivation of bacteria on solid stainless steel surfaces

Bacterial inactivation studies with 222 nm light on air-dried solid SS surfaces were carried on for all four foodborne pathogens, and the inactivation results are shown in Fig. 1b. All microbial counts decreased nonlinearly with increasing cumulative fluence. Interestingly, different bacterial responses to the treatment were observed in SS experiments compared to the TLF experiments. At the highest cumulative dose of 236 mJ/cm² (1000 s exposure), the most susceptible bacterium tested on solid SS substrates was L. monocytogenes, which was almost 4 times more susceptible than P. aeruginosa spread on SS surfaces, which was the least susceptible of all strains tested. A stronger correlation between susceptibility to 222 nm light and gram status was observed in SS experiments compared with the TLF experiments. After a cumulative dose of 236 mJ/ cm², two susceptibility clusters to 222 nm treatment were identified, with gram-negative E. coli (1.5 \pm 0.3 log reduction), P. aeruginosa (1.4 \pm 0.5 log reduction) in the more resistant cluster, and the gram-positive L. monocytogenes (5.1 \pm 0.5 log reduction), S. aureus (4.5 \pm 0.5 log reduction) in the more susceptible cluster. The reduction for all four strains was similar (P > 0.05) for a cumulative dose < 7.08 mJ/cm² (30 s exposure), but the susceptibility differences between the two clusters became significant (P < 0.05) starting at a cumulative fluence of 14.16 mJ/cm² (60 s exposure). In the lower susceptibility cluster, no significant difference in inactivation kinetics was observed between E. coli and P. aeruginosa throughout the entire treatment duration, and a long plateau was observed for both strains after 60 s of exposure up until the end of the 1000 s exposure (236 mJ/cm²). In the higher susceptibility cluster, both L. monocytogenes and S. aureus appeared to be very susceptible to 222 nm light, with no significant difference in the final inactivation levels between the two strains (P > 0.05) at the highest cumulative dose of 236 mJ/cm², and no pronounced plateau of the inactivation curves. All experimental inactivation data were fitted to the Weibull model, with all strains showing a good fit with the model (0.8 \leq $R^2 \leq 1.0$). The discrepancy in inactivation patterns between the TLF study and the SS study may be due to differences in the substrate conditions. In the surface treatments, more uniform exposure of the small volume of bacterial inoculum was achieved, whereas for the static liquid treatments light may have been partially blocked by the edges of the rectangularly shaped chamber, shielding some bacterial cells from the antimicrobial light. In a previous paper published by our group, Confocal microscopy images revealed that bacterial cells distribution varies significantly depending on the location within the suspending liquid (Cheng et al., 2020). When treating bacteria suspended in static TLFs, the cells on the bottom of the liquid suspension would receive lower light doses compared to the cells at the surface of the suspension, leading to nonuniformity in inactivation within the TLFs. Meanwhile, when bacteria were spread as droplets on the solid SS substrates, the bacterial population was more homogenously distributed on the surface of the SS coupons, allowing cells to receive a more even exposure to the incident 222 nm light compared with those in the TLF. These two distinct spatial distributions of the cells and the different light dose distribution in TLF suspensions vs. on solid SS substrates resulted in the variations in inactivation patterns in the two treatment scenarios, which was especially evident for E. coli.

Exposure to far-UV-C light was reported to induce biological damage mostly by affecting the cellular enzymes or membrane lipids because amino acids or phospholipids have an absorption peak around 222 nm wavelength (Ha et al., 2017; Oh, Sun, Araud, & Nguyen, 2020). Moreover, chromophores can generate ROS at this wavelength, which can significantly damage even DNA, even if DNA itself does not absorb UV radiation at 222 nm. Thus, 222 nm light can simultaneously affect

multiple cellular targets (Oh et al., 2020; Shin, Kim, & Kang, 2020). The consistently higher susceptibility to 222 nm of the gram-positive bacteria tested in this study suggests that different cell wall structures in gram-positive and -negative bacteria may impact the antibacterial effect this treatment substantially. It is possible that because of the low penetration ability of 222 nm light, the outer membrane in gramnegative bacteria may block some of the incident light from reaching lipoproteins and inner cell components, thus limiting the effectiveness of 222 nm treatment for these bacteria. Further studies are however needed to elucidate these mechanisms and the key factors influencing the antibacterial performance of 222 nm light against various classes of bacteria.

3.3. Bacteria resistance to far-UV-C treatments after serial exposure cycles

To provide a comprehensive evaluation of the disinfection potential of 222 nm light, this study also investigated the bacterial response after multiple cycles of exposure to check for the possible development of bacterial resistance, which could impact the effectiveness of such treatments and pose safety risks in applications in the long run (Shoults & Ashbolt, 2019). L. monocytogenes suspended in liquid BPB buffer was used to test for changes in resistance due to its consistent response to both the TLF and SS treatments. The number of exposure-growth cycles was chosen based on previous studies that reported changes in bacterial resistance (Alcántara-Díaz, Breña-Valle, & Serment-Guerrero, 2004; Ewing, 1995; Hartke, Giard, Laplace, & Auffray, 1998; Shoults & Ashbolt, 2019; Wright & Hill, 1968). Fig. 2 shows the results of 222 nm exposure delivered to L. monocytogenes at three different cumulative doses: 70.8 mJ/cm² (300 s exposure), 141.6 mJ/cm² (600 s exposure), and 236 mJ/cm² (1000 s exposure) over five exposure-growth cycles. No significant differences in log reductions were observed after the five serial exposure-growth cycles, regardless of light dose used. A linear regression analysis further indicated no declining trend in log reduction after repeated exposure (P > 0.05). However, larger variations in inactivation levels were observed after the higher dose (141.6 mJ/cm² and 236 mJ/cm²) treatments compared with the lower dose treatments (70.8 mJ/cm²). The greatest variability in final inactivation was observed in the 141.6 mJ/cm² cumulative fluence group, where the lowest reduction level (2.7 \pm 0.1 log) was seen after the fourth cycle and the highest reduction level (3.4 \pm 0.5 log) after the fifth cycle. Therefore, it is important to remain cautious in considering the applications of 222 nm treatments, especially when used at higher doses. Additionally, different bacteria may exhibit various environmental adaptations and resistance responses, hence more tests should be performed with application specific bacteria when implementing the far-UV-C technology.

3.4. Effect of 222 nm far-UV-C light on biofilm formation and growth

It is known that biofilm-bound cells are more resistant to bactericidal treatments than planktonic cells due to their extracellular matrix protection, poor penetration by light or chemicals, structural complexity, genetic up-regulation and metabolic heterogeneity (Liu et al., 2021). To investigate the effect of 222 nm light on biofilm formation and growth, the opportunistic pathogens and prolific biofilm formers *S. aureus* and *P. aeruginosa* were grown vertically on SS coupons for up to 48 h in TSB under the continuous exposure of 222 nm light. Three dimensional CLSM images of biofilm matrices at 24 h and 48 h and quantified biomass accumulations of *S. aureus* and *P. aeruginosa* are shown in Fig. 3.

For both S. aureus and P. aeruginosa, considerable biomass accumulation was found in the untreated dark control groups, which showed thick and dense bacteria layers and visible EPS matrices at both 24 h and 48 h. Compared with the dark controls, biomass accumulation for both strains was visibly reduced in the 222 nm light-treated groups, which also showed more sparse bacteria distribution and visibly less EPS matrix at 24 h and 48 h. At 24 h, the biomass accumulation for S. aureus grown in dark control was 15.4 \pm 1.5 $\mu m^3/\mu m^2$, while that in the lighttreated group was $2.2 \pm 1.1 \ \mu m^3 / \mu m^2$, amounting to a notable 86% average reduction in biomass. A consistent trend was observed at 48 h as well, with 66% less biomass accumulation observed for 222 nm lighttreated S. aureus compared with dark controls. The biomass accumulation of P. aeruginosa was similar to S. aureus and followed the same trend: 94% and 57% lower biomass accumulations were found in the treatment group compared with the untreated dark control at 24 h and 48 h, respectively. The lowest P. aeruginosa biomass accumulation was observed for 24 h light-treated samples $(0.8 \pm 0.3 \, \mu \text{m}^3/\mu \text{m}^2)$ and the highest biomass accumulation for the 48 h dark control samples (22.4 \pm 2.0 μm³/μm²). All differences in biomass accumulation between 222 nm light-treated bacteria and untreated controls were statistically significant (P < 0.05), which proves the biofilm growth inhibition effect of 222 nm light.

A closer analysis of the three dimensional biofilm structure further substantiated the differences in biofilm growth patterns between the light-treated and dark controls groups. The average volume of microcolonies attached to the substratum for both *S. aureus* and *P. aeruginosa* was calculated (Fig. S2 in the *Supplemental Information*). As the volume of microcolonies at substratum increases, bacterial colonization expands and leads to structured microbial communities and formation of a EPS matrix (Paula, Hwang, & Koo, 2020). For both *S. aureus* and *P. aeruginosa*, the average volume of microcolonies at substratum in the light-treated biofilms was smaller compared to the untreated biofilms, at

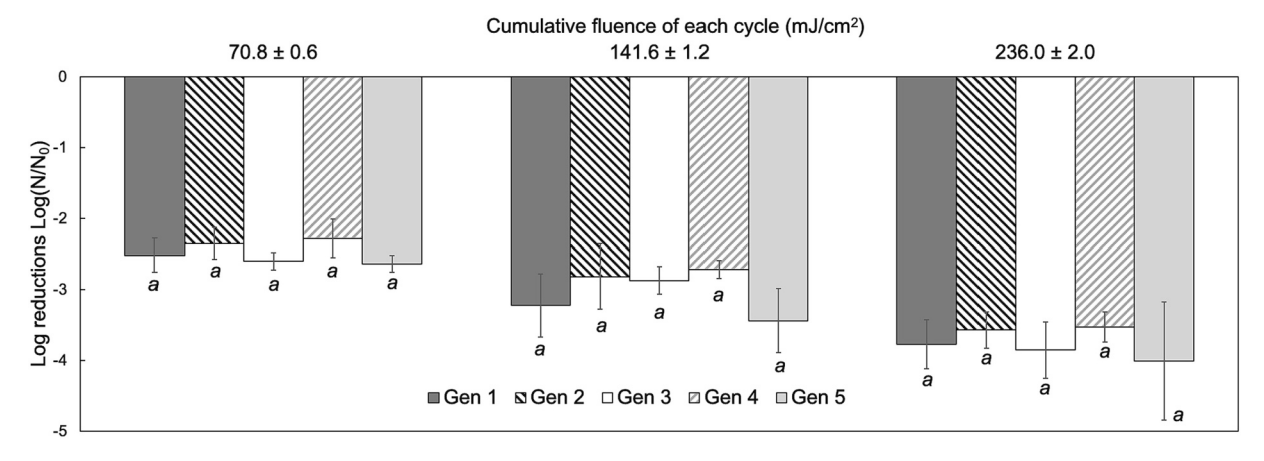


Fig. 2. Inactivation efficacy of 222 nm far-UV-C light against *L. monocytogenes* in thin liquid films over five serial exposure-growth cycles (5 generations of growth). Different letters denote significant differences (P < 0.05).

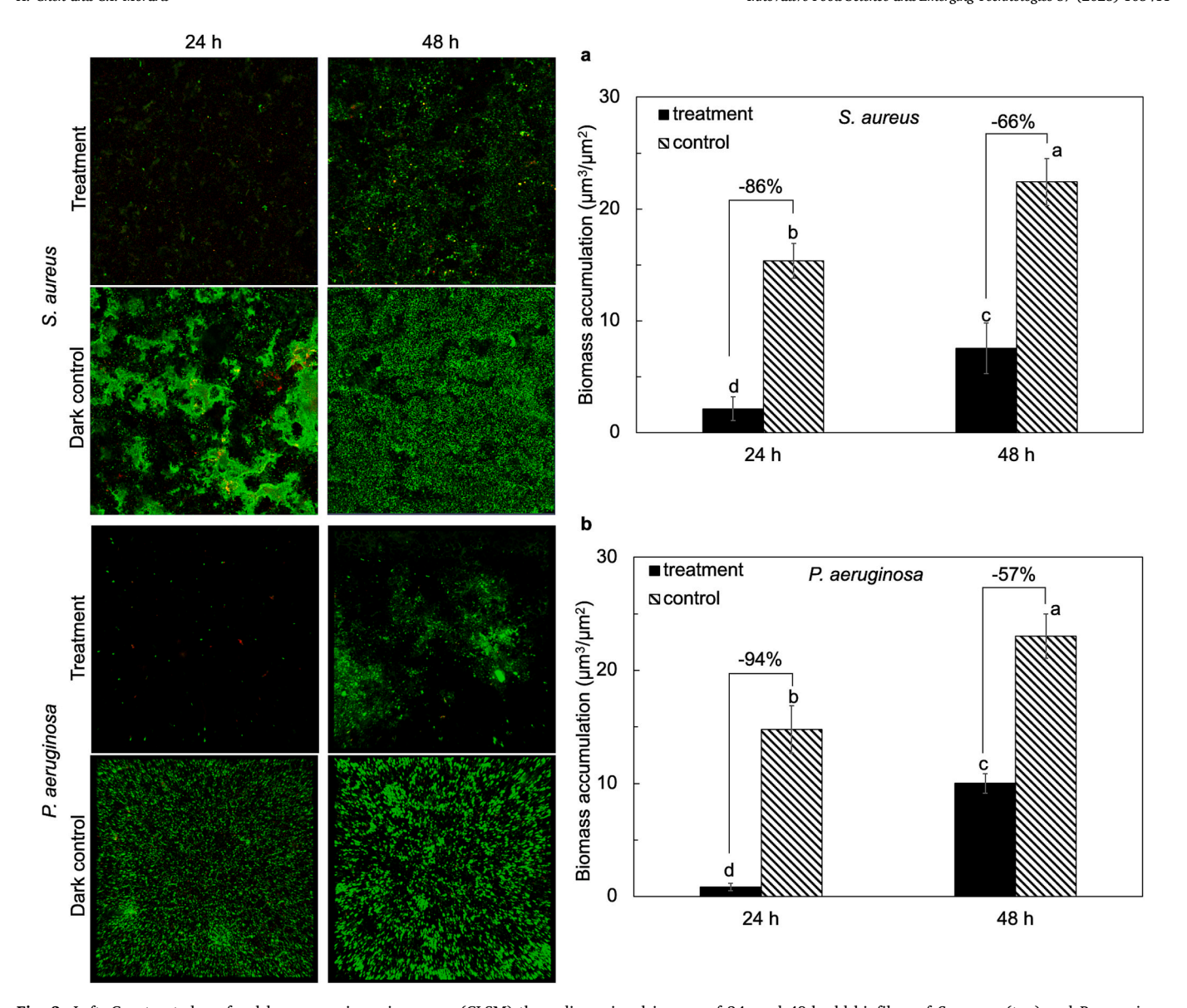


Fig. 3. Left: Constructed confocal laser scanning microscopy (CLSM) three-dimensional images of 24- and 48-h-old biofilms of *S. aureus* (top) and *P. aeruginosa* (bottom) on stainless steel surfaces without far-UV-C light exposure (control) and with far-UV-C light exposure during growth time. The presented images have biomass accumulation close to the average for their surface type, so that images are representative. Right: Differences in biomass accumulation (μ m³/ μ m²) over 24 h and 48h by *S. aureus* (a) and *P. aeruginosa* (b) between far-UV-C light treated and dark control groups. Values not connected by the same letter are statistically different from each other (P < 0.05). Error bars represent standard error of mean.

both 24 h and 48 h. Due to data variability, not all differences between light-treated and untreated biofilms were statistically significant (P > 0.05). Nonetheless, the consistent biofilm reduction trends shown in both biomass accumulation and volume of microcolonies at substratum show the effectiveness of continuous 222 nm light treatment against biofilm formation and growth on SS surfaces.

SEM imaging of bacterial cell morphology for both *S. aureus* and *P. aeruginosa* biofilms grown with and without the 222 nm light exposure are shown in Fig. 4, and the difference in cell attachments between light-treated and untreated groups are striking. As shown in Fig. 4, the untreated *S. aureus* cells were about 0.5 μ m in diameter and had a smooth and intact surface, with more prominent cell aggregation and extracellular matrix materials observed in the 48 h biofilm compared with the 24 h biofilm. For 24 h light-treated *S. aureus*, visibly less cells were attached to the SS surfaces, and their average cell diameters were slightly smaller, indicating the cells were not able to grow to maximum size (Hartmann et al., 2010). However, their surface morphology appeared unaltered. In the 48 h light-treated *S. aureus* biofilm, however,

cell surfaces appeared corrugated and cell shape slightly deformed. Similar trends were observed for *P. aeruginosa* cells, at both 24 h and 48 h time points. These SEM images allowed important observations of the cell attachment and potential cell injuries. To understand the active bactericidal effect of 222 nm lights and their impact on cell changes, more extensive characterization on cellular organelles and morphologies should be done in the future. In this study, for both *S. aureus* and *P. aeruginosa*, majority of the anti-biofilm properties from the 222 nm light should be credited to the anti-attachment and growth inhibition effects.

3.5. Chemical susceptibility of biofilm-bound cells that survived 222 nm light treatments

Light-treated S. aureus and P. aeruginosa cells from the biofilm study were soaked in 0.02 M sodium hypochlorite (NaClO) sanitizer for 1 min with continuous shaking at 21 $^{\circ}$ C to mimic manual mechanical action in cleaning and chemical sanitation procedures of surfaces in food

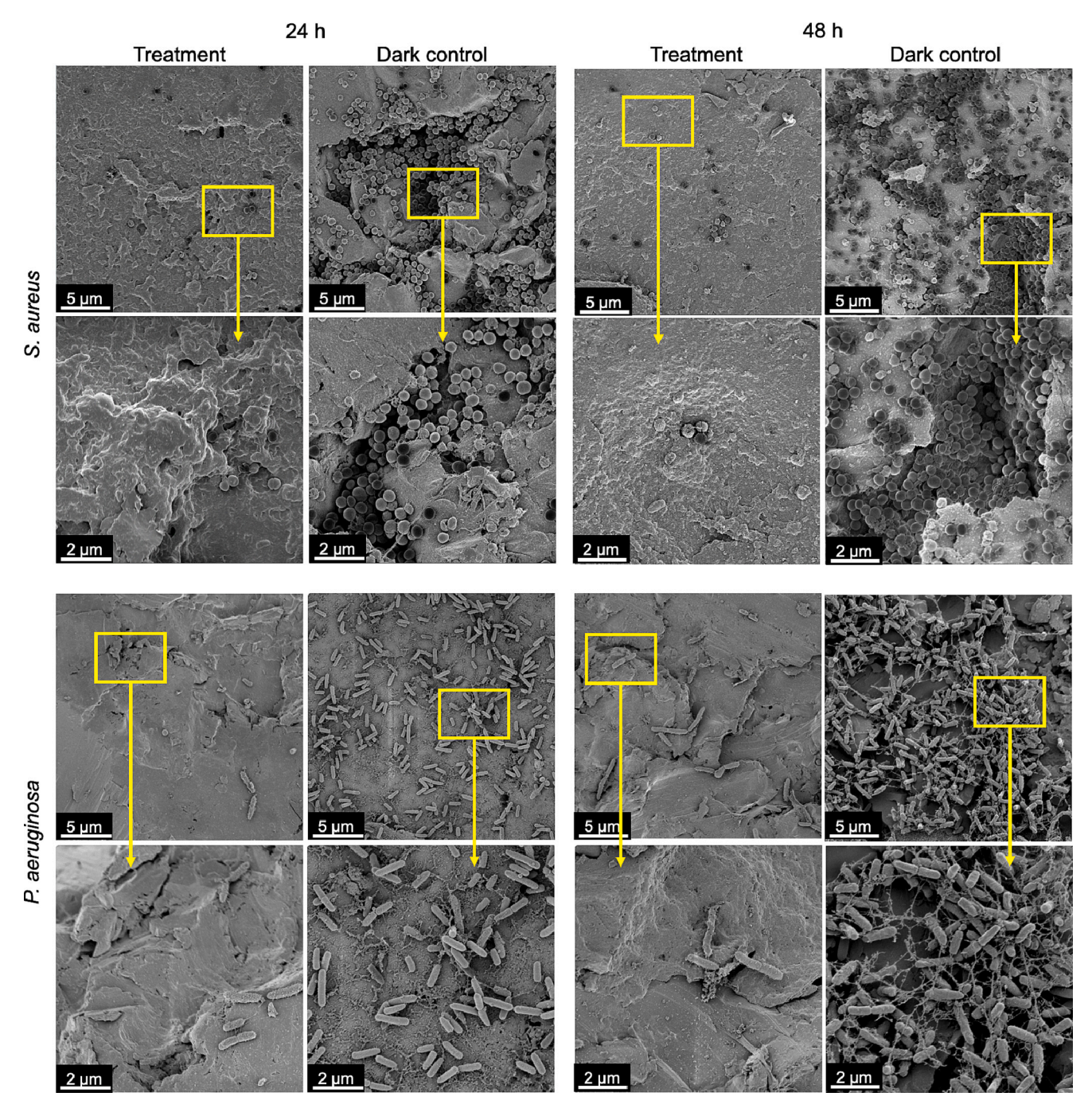


Fig. 4. Scanning electron microscopy images of *S. aureus* and *P. aeruginosa* at low magnification (upper) and high magnification (lower) after 24 h and 48 h far-UV-C light treatment and corresponding dark control groups during biofilm formation and growth on stainless steel surfaces.

processing and handling or clinical environments. The chemical susceptibility of S. aureus and P. aeruginosa cells after 222 nm light exposure increased significantly (P < 0.05) compared with untreated controls (Fig. 5). The 1 min soaking in NaClO sanitizer resulted in 1.6 ± 0.2 log reduction for light-treated S. aureus cells and only 0.5 ± 0.2 log reduction for untreated S. aureus cells, when the same starting concentration of cells was used (10^6 CFU/mL). Similarly, the light-injured P. aeruginosa cells were more readily inactivated in the 1 min NaClO sanitizer treatment, with up to 2 folds higher reduction achieved in light-treated P. aeruginosa (up to 0.1 ± 0.3 log reduction) compared with the untreated controls (up to 0.7 ± 0.1 log reduction). Different chemical susceptibility was also found between 24 h and 48 h light-treated cells: S. aureus and P. aeruginosa cells surviving 24 h light treatment were more

susceptible to the NaCIO sanitizer compared with 48 h light treated cells. This is likely because cells that were able to survive 48 h light treatments are much more resistant to environmental stressors and may exhibit resistance by developing various adaptation mechanisms (Li et al., 2021). Between the tested strains, *P. aeruginosa* were more susceptible to the NaClO sanitizer compared with *S. aureus*. Since gram-negative bacteria generally have greater antibiotic resistance than grampositive bacteria (Breijyeh, Jubeh, & Karaman, 2020), the high chemical susceptibility of the light-injured gram-negative *P. aeruginosa* cells suggest a potential application of 222 nm light as pre-treatment before chemical cleaning in various environments.

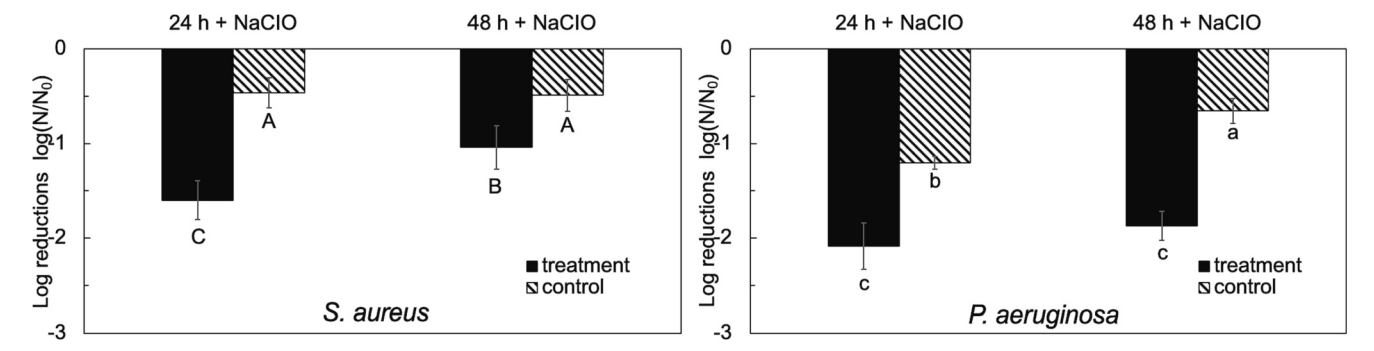


Fig. 5. Effect of 24 h and 48 h continuous exposure of 222 nm far-UV-C light on *S. aureus* (left) and *P. aeruginosa* (right) biofilm-bound cells grown on stainless steel surfaces on the subsequent chemical susceptibility to 0.02 M sodium hypochlorite (NaClO) sanitization. Values not connected by the same letter are statistically different from each other (P < 0.05). Error bars represent standard error of mean.

4. Conclusions

This work investigated the efficacy of 222 nm far-UV-C light emitted by a KrCl excilamp against gram-positive and gram-negative bacteria, both in liquid and on solid substrates. The experimental data demonstrated promising antimicrobial performance by the 222 nm light treatment for inactivating various planktonic pathogenic and spoilage bacteria. Additionally, no development of resistance was observed in *L. monocytogenes* after several exposure-growth cycles. This study also showed for the first time that 222 nm light can significantly inhibit biofilm formation and growth and improved the surviving cells' susceptibility to sodium hypochlorite sanitizer. These results advance the current knowledge about the antimicrobial effects of 222 nm far-UV-C technology and showed its potential for application as a nonthermal, non-hazardous treatment for mitigating microbial contamination in food processing or clinical environments.

Author information

Author Contributions: H.C.: conceptualization, data curation, formal analysis, investigation, methodology, writing - original draft, writing - reviewing and editing. C.I.M.: conceptualization, funding acquisition, project administration, supervision, resources, writing - reviewing and editing.

Declaration of Competing Interest

None.

Data availability

The datasets generated during and/or analyzed during the current study are available from the corresponding author on reasonable request.

Acknowledgements

This research was in part supported by the USDA, National Institute of Food and Agriculture, AFRI project 2022-67017-36289. This work made use of the Cornell Center for Materials Research (CCMR) shared facilities, supported through the NSF MRSEC program (DMR-1719875), and the Cornell University Biotechnology Resource Center (BRC) Imaging Facility (RRID:SCR_021741), with support from NIH 1S10RR025502 funding for the shared Zeiss LSM 710 Confocal Microscope. The authors thank Malcolm Thomas (CCMR), John Grazul (CCMR), and Johanna Dela Cruz (BRC) for their competent assistance.

Appendix A. Supplementary data

Supplementary data to this article can be found online at https://doi.org/10.1016/j.ifset.2023.103411.

References

Alcántara-Díaz, D., Breña-Valle, M., & Serment-Guerrero, J. (2004). Divergent adaptation of Escherichia coli to cyclic ultraviolet light exposures. *Mutagenesis*, 19, 349–354

Bjerkan, G., Witsø, E., & Bergh, K. (2009). Sonication is superior to scraping for retrieval of bacteria in biofilm on titanium and steel surfaces in vitro. Acta Orthopaedica, 80, 245–250.

Breijyeh, Z., Jubeh, B., & Karaman, R. (2020). Resistance of gram-negative Bacteria to current antibacterial agents and approaches to resolve it. *Molecules, 25*.

Buonanno, M., Welch, D., Shuryak, I., & Brenner, D. J. (2020). Far-UVC light (222nm) efficiently and safely inactivates airborne human coronaviruses. *Scientific Reports*, 10, 10285.

Cheng, Y., & Moraru, C. I. (2018). Long-range interactions keep bacterial cells from liquid-solid interfaces: Evidence of a bacteria exclusion zone near Nafion surfaces and possible implications for bacterial attachment. *Colloids and Surfaces. B, Biointerfaces*, 162, 16–24.

Cheng, Y., et al. (2020). Inactivation of Listeria and E. coli by Deep-UV LED: effect of substrate conditions on inactivation kinetics. Scientific Reports, 1–14. https://doi. org/10.1038/s41598-020-60459-8

Critzer, F., Science, F., Wszelaki, A., Ducharme, D., & Specialist, F. P. (2017). How to Use and Monitor Chlorine (Sodium / Calcium Hypochlorite) in Fruit and Vegetable Washwater and on Equipment and Food Contact Surfaces. 4.

Ewing, D. (1995). The directed evolution of radiation resistance in E. coli. *Biochemical and Biophysical Research Communications*, 216, 549–553.

Feng, G., et al. (2015). Bacterial attachment and biofilm formation on surfaces are reduced by small-diameter nanoscale pores: How small is small enough? npj Biofilms Microbiomes, 1.

Gayán, E., Condón, S., & Álvarez, I. (2013). Biological aspects in food preservation by ultraviolet light: A review. Food and Bioprocess Technology, 7, 1–20.

Ha, J. W., Lee, J. I., & Kang, D. H. (2017). Application of a 222-nm krypton-chlorine excilamp to control foodborne pathogens on sliced cheese surfaces and characterization of the bactericidal mechanisms. *International Journal of Food Microbiology*, 243, 96–102.

Hartke, A., Giard, J.-C., Laplace, J.-M., & Auffray, Y. (1998). Survival of enterococcus faecalis in an oligotrophic microcosm: Changes in morphology, development of general stress resistance, and analysis of protein synthesis. Applied and Environmental Microbiology, 64, 4238–4245.

Hartmann, M., et al. (2010). Damage of the bacterial cell envelope by antimicrobial peptides gramicidin S and PGLa as revealed by transmission and scanning electron microscopy. Antimicrobial Agents and Chemotherapy, 54, 3132–3142.

Hessling, M., Haag, R., Sieber, N., & Vatter, P. (2021). The impact of far-UVC radiation (200-230 nm) on pathogens, cells, skin, and eyes - a collection and analysis of a hundred years of data. GMS Hyg. Infection Control, 16. Doc07–Doc07.

Heydorn, A., et al. (2000). Quantification of biofilm structures by the novel computer program comstat. *Microbiology*, *146*, 2395–2407.

Janisiewicz, W., Takeda, F., Evans, B., & Camp, M. (2021). Potential of far ultraviolet (UV) 222 nm light for management of strawberry fungal pathogens. Crop Protection, 150, Article 105791.

Kang, J. W., Kim, S. S., & Kang, D. H. (2018). Inactivation dynamics of 222 nm kryptonchlorine excilamp irradiation on gram-positive and gram-negative foodborne pathogenic bacteria. Food Research International, 109, 325–333.

Kang, J.-W. H., & A.-J.-W. H. A.-D.-H. (2018). Effect of intermittent 222 nm kryptonchlorine excilamp irradiation on microbial inactivation in water. Food Control, 90, 146–151.

- Kim, D.-K., Kang, D.-H., & Schottel, J. L. (2018). UVC LED irradiation effectively inactivates aerosolized viruses, Bacteria, and Fungi in a chamber-type air disinfection system. Applied and Environmental Microbiology, 84. e00944–18.
- Li, H., et al. (2021). Decreased antibiotic susceptibility in Pseudomonas aeruginosa surviving UV Irradition. Frontiers in Microbiology, 12.
- Liu, Z., et al. (2021). Intense pulsed light for inactivation of foodborne gram-positive bacteria in planktonic cultures and bacterial biofilms. LWT, 152, Article 112374.
- Matafonova, G. G., Batoev, V. B., Astakhova, S. A., Gómez, M., & Christofi, N. (2008).
 Efficiency of KrCl excilamp (222 nm) for inactivation of bacteria in suspension.
 Letters in Applied Microbiology, 47, 508–513.
- Oh, C., Sun, P. P., Araud, E., & Nguyen, T. H. (2020). Mechanism and efficacy of virus inactivation by a microplasma UV lamp generating monochromatic UV irradiation at 222 nm. Water Research, 186, Article 116386.
- Paula, A. J., Hwang, G., & Koo, H. (2020). Dynamics of bacterial population growth in biofilms resemble spatial and structural aspects of urbanization. *Nature Communications*, 11, 1354.
- Rahmani, B., Bhosle, S., & Zissis, G. (2009). Dielectric-barrier-discharge Excilamp in mixtures of krypton and molecular chlorine. *Plasma Science IEEE Transactions*, 37, 546–550
- Shin, M., Kim, S.-S., & Kang, D.-H. (2020). Combined treatment with a 222-nm kryptonchlorine excilamp and a 280-nm LED-UVC for inactivation of salmonella typhimurium and Listeria monocytogenes. LWT, 131, Article 109715.

- Shoults, D. C., & Ashbolt, N. J. (2019). Decreased efficacy of UV inactivation of Staphylococcus aureus after multiple exposure and growth cycles. *International Journal of Hygiene and Environmental Health*, 222, 111–116.
- de Silerio-Vázquez, F. J., Núñez-Núñez, C. M., Proal-Nájera, J. B., & Alarcón-Herrera, M. T. (2022). A systematic review on solar heterogeneous photocatalytic water disinfection: Advances over time, operation trends, and prospects. *Catalysts*, 12.
- Uesugi, A. R., Woodling, S. E., & Moraru, C. I. (2007). Inactivation kinetics and factors of variability in the pulsed light treatment of Listeria innocua cells. *Journal of Food Protection*, 70, 2518–2525.
- Wang, D., Oppenländer, T., El-Din, M. G., & Bolton, J. R. (2010). Comparison of the disinfection effects of vacuum-UV (VUV) and UV light on Bacillus subtilis spores in aqueous suspensions at 172, 222 and 254 nm. Photochemistry and Photobiology, 86, 176–181.
- Welch, D., et al. (2018). Far-UVC light: A new tool to control the spread of airbornemediated microbial diseases. Scientific Reports, 8, 2752.
- Wright, S. J. L., & Hill, E. C. (1968). The development of radiation-resistant cultures of Escherichia coli 1 by a process of 'growth-irradiation cycles'. *Microbiology*, *51*, 97–106
- Yin, F., Zhu, Y., Koutchma, T., & Gong, J. (2015). Inactivation and potential reactivation of pathogenic Escherichia coli O157: H7 in apple juice following ultraviolet light exposure at three monochromatic wavelengths. Food Microbiology, 46, 329–335.